Progress In Electromagnetics Research C, Vol. 44, 251–261, 2013

TWO KINDS OF DUAL-BAND BANDPASS FILTER BASED ON A SINGLE SQUARE RING RESONATOR

Kun Deng *, Shou-Jia Sun, Shuai Yang, Bian Wu, and Chang-Hong Liang

National Laboratory of Science and Technology on Antennas and Microwaves, Xidian University, Xi'an, Shaanxi 710071, P. R. China

Abstract—In this paper, two kinds of dual-band bandpass filter (BPF) based on a single square ring resonator are presented, which are realized by loading capacitance or inductive stubs, respectively. Even-odd-mode analysis is applied to explain their model characteristics. One filter is implemented by loading a pair of capacitance stubs, and both in-band couplings can be tuned in a reasonable range. Another filter is completed by loading a pair of inductive stubs, and the first and second passband center frequencies can be controlled independently. For demonstration, two filters operating at 2.45/5.25 GHz and 2.4/5.25 GHz are designed and fabricated. The simulated and measured results show good agreements.

1. INTRODUCTION

Dual-band bandpass filter (BPF) has been a good candidate in recent wireless communication systems. Many reports about various dual-band bandpass filters (BPFs) have been published [1–6]. Among them, some dual-band BPFs are realized by employing two sets of resonators with different resonant frequencies [1–3], of which at least two resonators are needed and the filters occupy a large circuit size. The stepped impedance resonators (SIRs) and stub loaded resonators (SLRs) are also employed for dual-band operation [4–6], and at least two resonators are required. Other methods such as, defected ground structure (DGS) [7, 8], shorted-ended dual-mode resonator (SEDMR) [9], coupled line resonator [10], and low temperature co-fired ceramic (LTCC) [11] have also been proposed for dual-band applications.

Received 25 September 2013, Accepted 16 October 2013, Scheduled 17 October 2013

* Corresponding author: Kun Deng (dengkun139@gmail.com).

It is highly desirable to develop dual-band BPFs with compact size. The dual-band BPFs based on ring resonators have been attracting much more attention due to their compact size and good roll-off skirt [12–16]. In [12], two stub-loaded ring resonators are utilized to design dual-band BPF, as a result of this, the circuit size is larger than a single ring resonator BPF. Up to now, there are not so many reports on dual-mode dual-band filter using a single ring resonator [13–17]. In [17], a novel short-ended stepped-impedance dual-resonance resonator, which is evolved from SEDMR [9, 18], was proposed and applied to design filters with one, two, and three passbands. The resonator appears to be a ring, however, its working principle is equivalent to a stepped-impedance resonator (SIR) with two ends shorted. The resonant modes obtained from the resonator exhibit essential characteristics with those of SIR. The original short-ended resonator was proposed in [18], in order to realize miniaturization, the author connected the shorted ends together to be a ring shape. Although it looks like a ring resonator, it still works as a SIR with two ends shorted.

This paper presents two kinds of dual-band BPF, and both of them are stemmed from a single square ring resonator. One filter is implemented by loading a pair of capacitance stubs. Another one is designed by loading a pair of inductive stubs. As our best known, there are two degenerate orthogonal modes, TM_{10} and TM_{01}, coexisting in a symmetric ring resonator. In order to spilt these two degenerate modes, the internal coupling between the two resonant modes needs to be created by adding perturbations in a plane orthogonal to the ring [15]. The loaded stubs in this work are used to split the degenerate modes of the ring, which is different from those in [17]. Even-odd-mode method is used to analyze their model characteristics, according to which, each filter exhibits different features, in-band couplings or center frequencies of both passbands are controllable. In addition, the different feeding structures of both filters are discussed separately. For demonstration, two practical dual-band BPFs are designed and fabricated. The measured results validate the proposed design.

2. ANALYSIS OF THE SQUARE RING RESONATOR WITH LOADED STUBS

Figure 1(a) and Figure 2(a) show the Resonators I and II respectively, which are based on square ring resonators. The unique difference between them is the different types of loaded stubs at the plane P-P', and it is a pair of capacitance stubs in Resonator I and a pair of inductive stubs in Resonator II. The perturbation along the symmetry

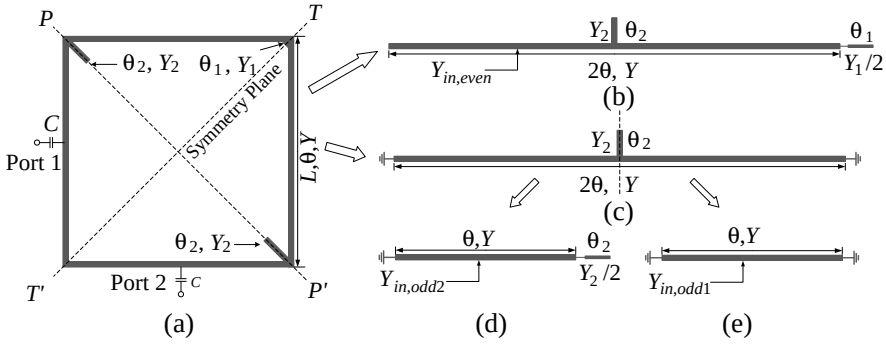

Figure 1. (a) Schematic of the proposed Resonator I. (b) Even- and (c) odd-mode equivalent circuit of (a). (d) Even- and (e) odd-mode equivalent circuit of (c).

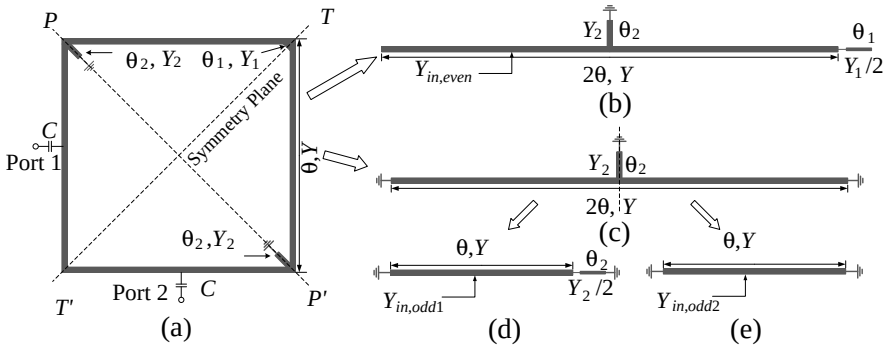

Figure 2. (a) Schematic of the proposed Resonator II. (b) Even- and (c) odd-mode equivalent circuit of (a). (d) Even- and (e) odd-mode equivalent circuit of (c).

plane T-T' in each resonator can be equivalent to a transmission line with an effective electrical length of θ_1 and a admittance of Y_1. Due to different types of loaded stubs, two resonators exhibit different properties.

2.1. Resonator I with Loaded Capacitance Stubs

As shown in Figure 1(a), a pair of capacitance stubs with electrical length θ_2 and admittance Y_2 is loaded at the plane P-P'. Meanwhile, the perturbation with electrical length θ_1 and admittance Y_1 is loaded at the symmetry plane T-T'. Even-odd-mode method is employed

to analyze its resonant properties, Figure 1(b) and Figure 1(c) show the even- and odd-mode equivalent circuits respectively. In order to facilitate analysis, $Y_1 = Y_2 = Y$. According to the resonant condition $\mathrm{Im}\{Y_{in}\} = 0$, it can be deduced from Figure 1(b) that

$$\tan\theta \cdot (4 - \tan\theta_1 \cdot \tan\theta_2) + \tan\theta_1 \left(1 - \tan^2\theta\right) + 2\tan\theta_2 = 0 \quad (1)$$

The circuit in Figure 1(c) is still symmetrical, and even-odd-mode analysis is applied once again to explain its resonant characteristics. Figure 1(d) and Figure 1(e) depict the even- and odd-mode equivalent circuits of Figure 1(c) respectively, and their resonant condition can be derived as

$$\tan\theta \cdot \tan\theta_2 - 2 = 0 \quad (2)$$

$$\theta = \pi \quad (3)$$

Two resonant frequencies can be obtained from (1), and another two resonant frequencies can be deduced from (2) and (3), respectively. Meanwhile, once the perimeter of the square ring resonator is fixed, the resonant frequency derived from (3) keeps constant. Here, two variables a_1 and a_2 are defined as:

$$a_1 = \frac{\theta_1}{\theta} \quad \text{and} \quad a_2 = \frac{\theta_2}{\theta} \quad (4)$$

Figure 3 shows the variations of the resonant frequencies against a_2. Among them, f_2 and f_3 are derived from (1), and f_1 and f_4 are stemmed from (2) and (3) respectively. There are five conclusions can be obtained from Figure 3:

1) f_1 and f_2 will form a passband with center frequency $f_{01} = (f_1 + f_2)/2$, and f_3 and f_4 will constitute another passband with center frequency $f_{02} = (f_3 + f_4)/2$;

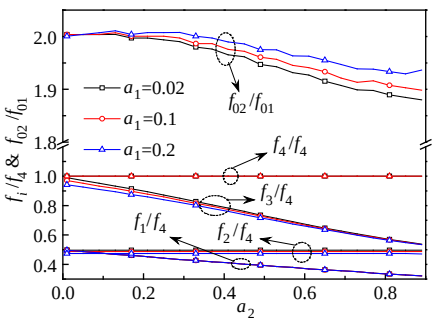

Figure 3. The variations of frequencies ratios against a_1 and a_2.

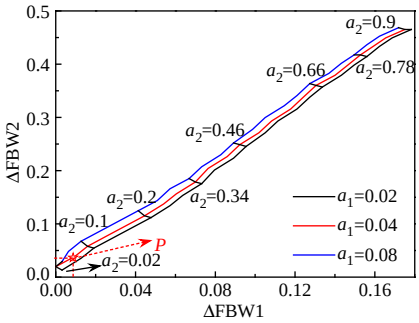

Figure 4. Design graph of the proposed resonator I.

2) The variation of a_2 changes f_1 and f_3, while there is no influence on f_2 and f_4;
3) The variation of a_1 changes f_2 and f_3, while there is no influence on f_1 and f_4;
4) Both a_1 and a_2 will affect f_{02}/f_{01};
5) When a_2 changes from 0 to 1, there are always some cases that f_2 is less than f_1 except the condition that $a_1 = a_2 = 0$.

In practical dual-band BPF design, when f_2 is less than f_1, both passband performance is poor, so in order to solve the problem, the variation ranges of a_1 and a_2 are defined as follows: $0.02 \leq a_1 \leq 0.08$ and $a_2 \geq 0.02$. In addition, when a_2 is too large, both passband bandwidths are too wide to supply sufficient external coupling, therefore, $a_2 \leq 0.2$ is chosen. Due to the above constraints, it can be observed from Figure 3 that, the center frequency ratio f_{02}/f_{01} is approximately equal to 2 and not controllable, which is the main drawback in dual-band BPF design utilizing Resonator I. Now, in-band couplings of both passbands are the only one parameter that can be controllable. Figure 4 demonstrates the design graph of the proposed Resonator I, in which ΔFBW1 and ΔFBW2 represent the in-band couplings of both passbands and they are defined as

$$\Delta\text{FBW1} = (f_2 - f_1)/f_4 \quad \text{and} \quad \Delta\text{FBW2} = (f_4 - f_3)/f_4 \tag{5}$$

Since fractional bandwidth is related with resonant frequencies, thus it can be known from Figure 4 that both bandwidths can be controlled with different in-band couplings by tuning a_1 and a_2.

2.2. Resonator II with Loaded Inductive Stubs

Schematic layout of Resonator II is shown in Figure 2(a), the difference from Resonator I is that a pair of inductive stubs realized by shorted-stub is loaded at the plane P-P'. The resonant conditions can be derived from its equivalent circuits shown in Figure 2(b), Figure 2(d) and Figure 2(e), and they are demonstrated as follows

$$\tan\theta \cdot (\tan\theta_1 + 4\tan\theta_2) + \tan\theta_1 \cdot \tan\theta_2 \left(1 - \tan^2\theta\right) - 2 = 0 \quad \text{for Figure 2(b)} \tag{6}$$

$$\tan\theta + 2\tan\theta_2 = 0 \quad \text{for Figure 2(d)} \tag{7}$$

$$\theta = \pi \quad \text{for Figure 2(e)} \tag{8}$$

$$a_1 = \frac{\theta_1}{\theta} \quad \text{and} \quad a_2 = \frac{\theta_2}{\theta} \tag{9}$$

According to (6)–(9), Figure 5 illustrates the variations of resonant frequencies and both passbands in-band couplings against a_2 under different values of a_1. Among them, f_1 and f_2 are obtained from (6),

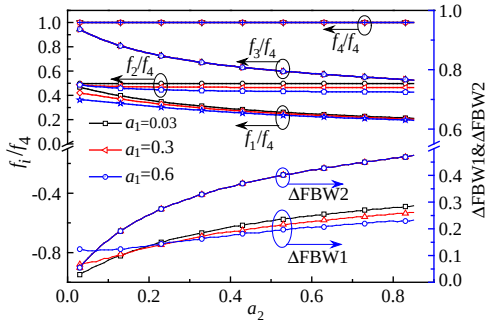

Figure 5. The variations of frequencies and in-band couplings against a_2.

and f_3 and f_4 are deduced from (7) and (8) respectively. In addition, the definitions of ΔFBW1 and ΔFBW2 are the same as mentioned in (5). Two conclusions can be obtained from Figure 5: First, the variation of a_2 affects f_1 and f_3, and there is almost no influence on f_2 and f_4, i.e., a_2 will control both passband in-band couplings during the dual-band BPF design procedure; Second, a_1 changes f_1 and f_2, and have no effect on f_3 and f_4, i.e., the first passband center frequency can be individually controlled via a_1.

Up to now, both passbands center frequencies of the dual-band BPF utilizing Resonator II are independent of each other.

2.3. I/O Coupling Scheme

Figure 6 shows two I/O coupling schemes of Resonators I and II. Two ports are perpendicular in Scheme I, and parallel in Scheme II. With weak coupling excitations, the transmission responses of Figures 6(a) and (b) are plotted in Figures 7(a) and (b), respectively. The software Zeland IE3D is employed for the simulation. From Figure 7(a), there is a transmission zero between two poles of each passband for Scheme II, which destroys the passband property and is unavailable. Scheme I is more suitable for Resonator I, since there are two transmission zeros located at passband edges, which enhances passband selectivity. In addition, another one transmission zero between two passbands improves the band-to-band isolation. The I/O coupling scheme of Resonator II is different from that of Resonator I, as shown in Figure 7(b), Scheme II is more suitable for Resonator II rather than Scheme I.

At last, the conclusion is that, in dual-band BPF design, I/O coupling Scheme I is employed for Resonator I, and I/O coupling Scheme II is used for Resonator II.

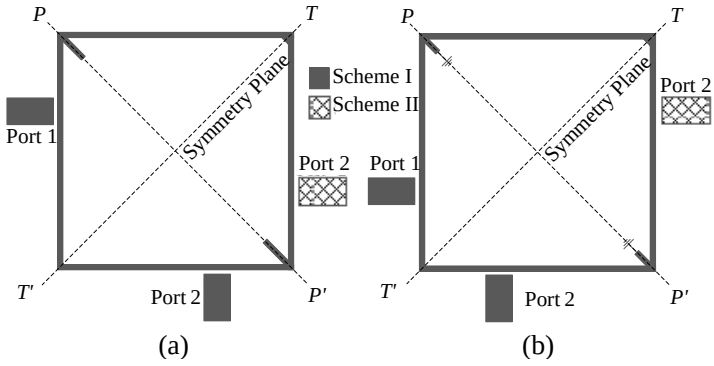

Figure 6. Two I/O coupling schemes of (a) resonator I and (b) resonator II.

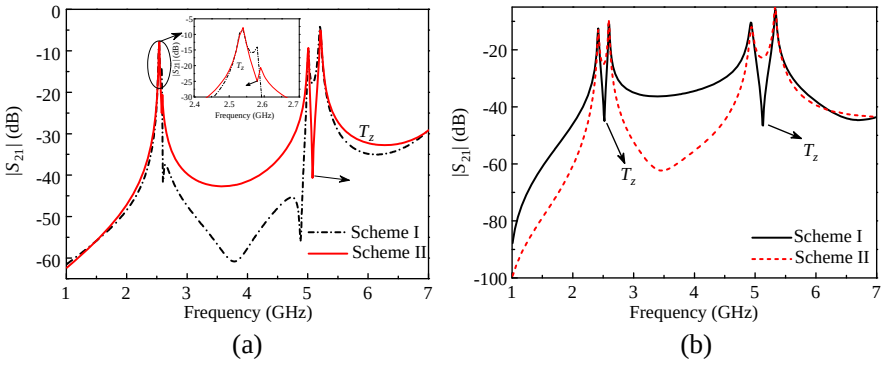

Figure 7. (a) and (b) Transmission responses of Figures 6(a) and (b).

3. FILTER DESIGN, FABRICATION AND MEASUREMENT

3.1. Filter Configuration

Figures 8(a) and (b) show the configuration of the proposed dual-band bandpass filter with Resonator I and Resonator II, respectively. Parallel-Coupled microstrip lines (PCML) are used to provide external quality factor for both filters.

3.2. Filter Design Procedure

Based on the above analysis, the design procedures of the presented dual-band BPF can be summarized as follows. First, obtain desired

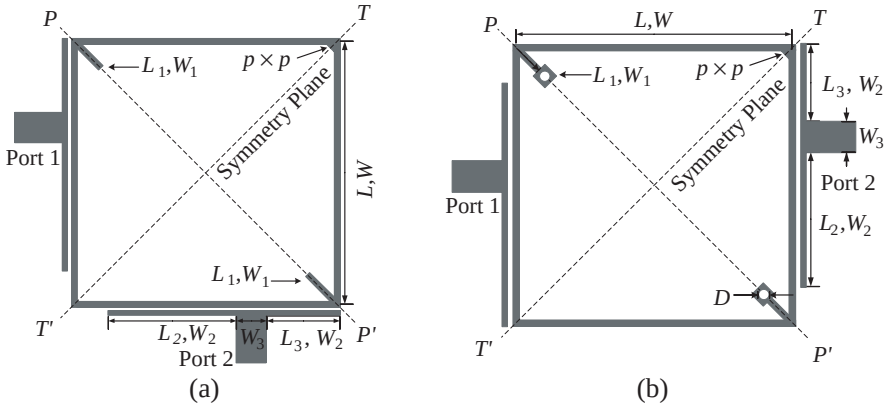

Figure 8. Circuit layouts of (a) filter I and (b) filter II.

passband frequencies. Suitable resonator type should be selected in this step. The second step is to achieve required bandwidth for each passband. The bandwidth depends on the external quality factor and coupling coefficients. The coupling coefficients are determined by the loaded stub length. The external quality factor depends on the coupling gap and line length of the coupled port line.

After the preceding two steps, the initial dimensions of the filter can be obtained. Finally, fine tuning can be performed to meet the specifications at both passbands.

3.3. Simulation and Measurement Results

To verify the proposed concept, two filters are optimally designed using full-wave electromagnetic (EM) simulator IE3D and fabricated on a dielectric substrate with a thickness of $h = 1\,\text{mm}$ and a dielectric constant of $\varepsilon_r = 2.65$. Figures 9(a) and (b) depict the fabricated photographs of the two filters in Figures 8(a) and (b), respectively. Comparisons of simulated and measured results of filter I and filter II are shown in Figures 10(a) and (b), respectively. The measured results show that, two bands of filter I in Figure 9(a) center at 2.45 and 5.28 GHz, with the corresponding bandwidths of 6.1% and 10.2%, insertion losses less than 1.3 and 1.4 dB, return losses more than 14.4 and 18.3 dB.

The measured center frequencies of filter II in Figure 9(b) are 2.42 and 5.24 GHz, respectively. The fractional bandwidths of the two passbands are found to be 7.4% and 9.2%, respectively. The measured minimum insertion loss is around 1.8 dB in the first passband and is

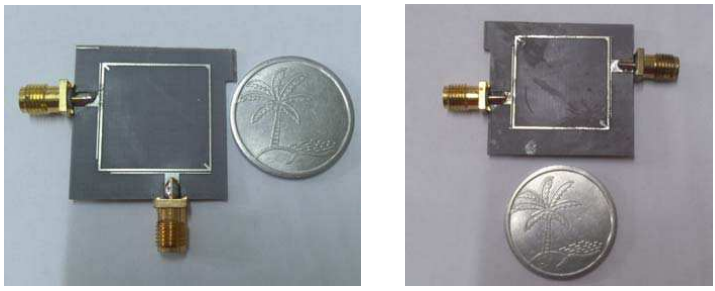

(a) (b)

Figure 9. Fabricated photographs of (a) Filter I, the dimensions are: $L = 21.6$, $L_1 = 1.16$, $L_2 = 10.6$, $L_3 = 6.3$, $W = 0.5$, $W_1 = 0.5$, $W_2 = 0.3$, $W_3 = 2.73$, $p = 0.71$, and (b) filter II, the dimensions are: $L = 21.2$, $L_1 = 0.88$, $L_2 = 9.1$, $L_3 = 5.1$, $W = 0.5$, $W_1 = 0.5$, $W_2 = 0.3$, $W_3 = 2.73$, $p = 0.71$, $D = 1$ (in mm).

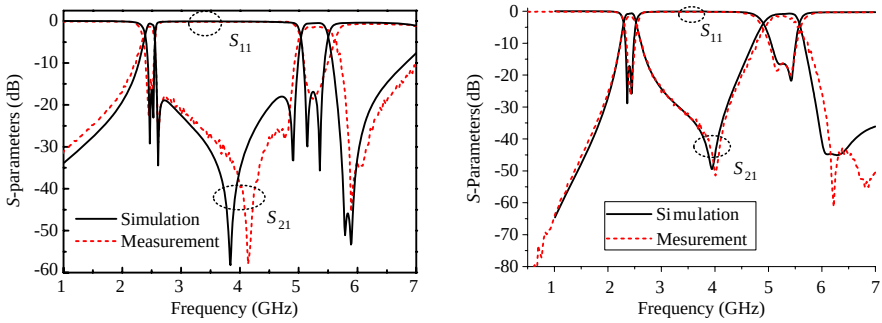

(a) (b)

Figure 10. Comparisons of simulated and measured frequency response. (a) Filter I. (b) Filter II.

around 1.53 dB in the second passband. The return loss is better than 17.4 and 16.1 dB in most of the first and second passband, respectively.

4. CONCLUSION

Two kinds of dual-band bandpass filter based on a single square ring resonator are presented in this paper. By loading different loaded stubs, distinct characteristics are found and discussed. Experimental circuits are fabricated and measured to validate the design concept. Measured results show that the proposed filters are suitable for WLAN applications.

ACKNOWLEDGMENT

This work was supported by the National High Technology Research and Development Program of China (863 Program) No. 2012AA01A308 and the National Natural Science Foundation of China (NSFC) under Project Nos. 61271017 and 61072017.

REFERENCES

1. Xu, F., Z.-J. Wang, M. Xiao, J.-Z. Duan, J.-Y. Cui, Z. Zhu, M. Ju, and Y. Liu, "A compact dual-band band-pass filter with wide stop-band using two resonators combined by via-hole," *Progress In Electromagnetics Research C*, Vol. 41, 81–95, 2013.
2. Jia, D.-H., Q.-Y. Feng, X.-G. Huang, and Q.-Y. Xiang, "A dual-band bandpass filter with a tunable passband," *Progress In Electromagnetics Research C*, Vol. 37, 107–118, 2013.
3. Kuo, J.-T. and S.-W. Lai, "New dual-band bandpass filter with wide upper rejection band," *Progress In Electromagnetics Research*, Vol. 123, 371–384, 2012.
4. Huang, X.-G., Q.-Y. Feng, Q.-Y. Xiang, and D.-H. Jia, "A high selectivity dual-band bandpass filter using dual-mode and triple-mode resonators," *Progress In Electromagnetics Research C*, Vol. 36, 81–90, 2013.
5. Xu, J. and W. Wu, "Compact microstrip dual-mode dual-band band-pass filters using stubs loaded coupled line," *Progress In Electromagnetics Research C*, Vol. 41, 137–150, 2013.
6. Wu, Y.-L., C. Liao, X.-Z. Xiong, and X.-M. Zhong, "Design filters using tunable E-shaped dual-mode resonators for lower-ultra-wideband and upper-ultra-wideband applications," *Progress In Electromagnetics Research C*, Vol. 37, 145–157, 2013.
7. Wang, Z.-D., F. Wei, L. Zhang, and X.-W. Shi, "Compact tunable dual-band bandpass filter based on substrate integrated waveguide and defected ground structure," *Progress In Electromagnetics Research Letters*, Vol. 41, 193–203, 2013.
8. Li, Y., H.-C. Yang, and S.-Q. Xiao, "Design of dual band filter based on a novel DGS structure," *Progress In Electromagnetics Research Letters*, Vol. 41, 167–174, 2013.
9. Sun, S.-J., S. Yang, B. Wu, K. Deng, and C.-H. Liang, "Dual-band bandpass filter using a single short-ended dual-mode resonator with adjustable first passband," *Progress In Electromagnetics Research C*, Vol. 37, 95–106, 2013.

10. Kuo, J.-T., C.-Y. Fan, and S.-C. Tang, "Dual-wideband bandpass filters with extended stopband based on coupled-line and coupled three-line resonators," *Progress In Electromagnetics Research*, Vol. 124, 1–15, 2012.
11. Zhou, C.-X., Y.-X. Guo, L. Wang, and W. Wu, "Design of compact dual-band filter in multilayer LTCC with cross coupling," *Progress In Electromagnetics Research*, Vol. 135, 515–525, 2013.
12. Deng, K., S. Yang, S.-J. Sun, B. Wu, and X.-W. Shi, "Dual-mode dual-band bandpass filter based on square loop resonator," *Progress In Electromagnetics Research C*, Vol. 37, 119–130, 2013.
13. Liu, Y., H.-X. Zheng, and L.-Y. Feng, "A compact dual-mode resonator with square loops and its bandpass filter applications," *Progress In Electromagnetics Research Letters*, Vol. 41, 51–61, 2013.
14. Liu, J.-C., F.-S. Huang, C.-P. Kuei, and C.-Y. Liu, "Compact dual-mode double square-loop resonators for WLAN and WiMAX tri-band filter design," *Progress In Electromagnetics Research C*, Vol. 38, 101–113, 2013.
15. Luo, S., L. Zhu, and S. Sun, "A dual-band ring-resonator bandpass filter based on two pairs of degenerate modes," *IEEE Trans. Microw. Theory Tech.*, Vol. 58, No. 12, 3427–3432, 2010.
16. Huang, T.-H., H.-J. Chen, C.-S. Chang, L.-S. Chen, Y.-H. Wang, and M.-P. Houng, "A novel compact ring dual-mode filter with adjustable second passband for dual-band applications," *IEEE Microw. Wireless Compon. Lett.*, Vol. 16, No. 6, 360–362, 2006.
17. Sun, S.-J., T. Su, K. Deng, B. Wu, and C.-H. Liang, "Shorted-ended stepped-impedance dual-resonance resonator and its application to bandpass filter," *IEEE Trans. Microw. Theory Tech.*, Vol. 61, No. 9, 3209–3215, 2013.
18. Sun, S.-J., B. Wu, T. Su, K. Deng, and C.-H. Liang, "Wideband dual-mode microstrip filter using short-ended resonator with centrally loaded inductive stub," *IEEE Trans. Microw. Theory Tech.*, Vol. 60, No. 12, 3667–3673, 2012.